

## RESEARCH ARTICLE

# Gene expression profiling of proximal and distal renal tubules in Atlantic salmon (*Salmo salar*) acclimated to fresh water and seawater

Steffen S. Madsen,<sup>1</sup> Rebecca J. Bollinger,<sup>1</sup> Melanie Brauckhoff,<sup>1</sup> and Morten Buch Engelund<sup>2</sup>

<sup>1</sup>Department of Biology, University of Southern Denmark, Odense M, Denmark; and <sup>2</sup>Department of Clinical Genetics, Odense University Hospital, Odense M, Denmark

Submitted 2 December 2019; accepted in final form 1 July 2020

**Madsen SS, Bollinger RJ, Brauckhoff M, Engelund MB.** Gene expression profiling of proximal and distal renal tubules in Atlantic salmon (*Salmo salar*) acclimated to fresh water and seawater. *Am J Physiol Renal Physiol* 319: F380–F393, 2020. First published July 6, 2020; doi:10.1152/ajprenal.00557.2019.—Euryhaline teleost kidneys undergo a major functional switch from being filtratory in freshwater (FW) to being predominantly secretory in seawater (SW) conditions. The transition involves both vascular and tubular effects. There is consensus that the glomerular filtration rate is greatly reduced upon exposure to hyperosmotic conditions. Yet, regulation at the tubular level has only been examined sporadically in a few different species. This study aimed to obtain a broader understanding of transcriptional regulation in proximal versus distal tubular segments during osmotic transitions. Proximal and distal tubule cells were dissected separately by laser capture microdissection, RNA was extracted, and relative mRNA expression levels of >30 targets involved in solute and water transport were quantified by quantitative PCR in relation to segment type in fish acclimated to FW or SW. The gene categories were aquaporins, solute transporters, fxyd proteins, and tight junction proteins. *aqp8bb1*, *aqp10b1*, *nhe3*, *sglt1*, *slc41a1*, *cnm3*, *fxyd12a*, *cldn3b*, *cldn10b*, *cldn15a*, and *cldn12* were expressed at a higher level in proximal compared with distal tubules. *aqp1aa*, *aqp1ab*, *nka-a1a*, *nka-a1b*, *nkcc1a*, *nkcc2*, *ncc*, *clc-k*, *slc26a6C*, *sglt2*, *fxyd2*, *cldn3a*, and *ocln* were expressed at a higher level in distal compared with proximal tubules. Expression of *aqp1aa*, *aqp3a1*, *aqp10b1*, *ncc*, *nhe3*, *cftr*, *sglt1*, *slc41a1*, *fxyd12a*, *cldn3a*, *cldn3b*, *cldn3c*, *cldn10b*, *cldn10e*, *cldn28a*, and *cldn30c* was higher in SW- than in FW-acclimated salmon, whereas the opposite was the case for *aqp1ab*, *slc26a6C*, and *fxyd2*. The data show distinct segmental distribution of transport genes and a significant regulation of tubular transcripts when kidney function is modulated during salinity transitions.

ion transport; kidney; tubular dynamics; water transport

## INTRODUCTION

The osmoregulatory challenges and mechanisms involved in maintaining homeostasis are to a large degree shared between different teleost species. In freshwater (FW), teleosts experience passive loss of ions and osmotic influx of water from the dilute surroundings. In seawater (SW), dehydration and passive ion load are experienced. Thus euryhaline teleosts must be capable of switching between hyper- and hypo-osmoregulation when traveling from FW to SW. Osmotic homeostasis is regulated by three primary organs: gill, gastrointestinal (GI) tract, and kidney. In FW, the gill is the main site of active compensatory uptake of ions from the environment (31, 44),

while the intestine may supplement with ions from the food (79). The glomerular kidney is designed to rid excess water while reabsorbing solutes and produces significant volumes of strongly hypotonic urine (63). In SW, compensation for dehydration is obtained through the ingestion and absorption of ambient water in the GI tract. Osmotic absorption of water, however, is solute based, thus adding to the total load of monovalent ions. Subsequently, these ions are primarily excreted by the gill (42, 82), while divalent ions such as  $Mg^{2+}$  and  $SO_4^{2-}$  are actively excreted in a strongly reduced volume of isotonic urine (9). Thus euryhaline teleosts make major adjustments in renal function as the salinity changes (8).

The teleost kidney is poorly organized compared with its mammalian counterpart. Vasculature, glomeruli, and tubular segments are intermingled with hematopoietic tissue and gives the overall impression of a disordered three-dimensional structure (5, 73). It lacks a well-defined zonation and loops of Henle and is accordingly limited to producing hypo- to isotonic urine. The number and size of glomeruli and the differentiation of tubular segments vary according to evolutionary origin of teleosts. As extreme examples, some species completely lack glomeruli, and truly marine species generally lack the distal segment of the nephron (41). In salmon, blood is filtered into Bowman's capsule preceding proximal tubule segments I and II, followed by distal and collecting tubules and collecting ducts. The urine enters the paired mesonephric ducts, which merge to form the urinary bladder, from where it is discharged through the urinary papilla. Each tubular segment as well as the urinary bladder makes its contribution to modify the filtrate toward its final composition (41). Katoh et al. (50) estimated that in rainbow trout, the relative contribution of proximal and distal segments to total nephron length was 30 and 63%, respectively.

The function of the proximal segments is somewhat controversial. Regarding NaCl and water transport, there is evidence in some species that the proximal segments of both FW and SW fish are responsible for transcellular absorption of  $Na^+$  and  $Cl^-$  as well as glucose and other important osmolytes (8, 23, 67). The mechanism for this builds on the expression of yet undefined isoforms of basolateral  $Na^+K^+$ -ATPase (NKA) (50, 80). The apical  $Na^+$  entry into proximal cells is yet unclear but may involve  $Na^+/H^+$  exchange [ $Na^+/H^+$  exchanger 3 (NHE3) (12, 47)] as well as  $Na^+$ /glucose cotransporters (SGLT, solute-carrier family 5, *slc5a*). Renal SGLT proteins have not been investigated in teleosts, but they have been demonstrated in cartilaginous fishes (2, 3). There is evidence that the absorptive-type  $Na^+K^+-2Cl^-$ -cotransporter (NKCC2,

Correspondence: S. S. Madsen (steffen@biology.sdu.dk).

Slc12a1) is absent in this segment (50) similar to mammals. In accordance with the mammalian model, it was earlier suspected that some water absorption occurred in the proximal segments driven by a locally established osmotic gradient (41). This model may, however, be challenged by the presence of basolateral secretory-type NKCC1 (Slc12a2) at least in killifish (*Fundulus heteroclitus*) (50), which suggests a pathway for NaCl secretion in conjunction with  $Mg^{2+}$  secretion and thus facilitating water secretion in the proximal segment (8). Trans-epithelial movement of water nonetheless requires appropriate expression of aquaporins and/or tight junction claudin proteins to facilitate trans- or paracellular transport, respectively.

In contrast to NaCl, there is consensus that one primary function of the proximal segment is secretion of  $Mg^{2+}$  and  $SO_4^{2-}$ , especially needed in SW-acclimated conditions.  $Mg^{2+}$  secretion involves apical exocytosis of vesicles enriched with  $Mg^{2+}$  by the magnesium transporter Slc41a1 (46, 47, 72). Another metal transporting protein, cyclin and CBS domain divalent metal cation transport mediator 3 (CNNM3), has been demonstrated in euryhaline mufugu (*Takifugu obscurus*) proximal tubule basolateral membranes, where, although not yet confirmed, it has been proposed to establish a paracellular  $Mg^{2+}$  gradient (45). Fluid secretion may follow in both filtering and nonfiltering nephrons, particularly in SW fish to facilitate  $Mg^{2+}$  secretion in tubules with low glomerular filtration rates. In FW,  $Mg^{2+}$  secretion is expected to be low but could play an additional role in excretion of excess water (8).

Distal tubules and collecting ducts together make up a variable percentage of whole nephron length in different fishes (50). NaCl reabsorption is the dominating process in both FW and SW, hence the name “diluting segment” (68). This is mediated by extensive basolateral NKA, apical NKCC2, and NaCl cotransporter (NCC, Slc12a3) (49, 50) and basolateral kidney-specific  $Cl^-$  channels (ClC-K) (66). In FW fish, the distal segments must have low water permeability to minimize water reabsorption (63, 68). Upon SW acclimation, the fractional reabsorption of water increases along the nephron by increasing tubular water permeability. Reabsorption of NaCl promotes the osmotic removal of water, thereby creating isotonic urine primarily consisting of  $MgSO_4$  and other unwanted solutes (8).  $Mg^{2+}$  reabsorption has been speculated to occur in the distal segment/collecting duct cells of killifish based on observations of Mg accumulation in these cells after a load of radioactive  $Mg^{2+}$  (18), but the mechanism has not been explored.

For the mammalian kidney, it is known that in addition to the highly segment-specific expression of ion- and water-transporting proteins, critical changes in the permeability properties defined by the differential expression and combination of tight junction claudin proteins occur along the nephron (40, 43). In fishes, >35 claudins have been reported in the kidney, and some of these are regulated in response to salinity (52). It is generally expected that overall ionic paracellular permeability decreases from proximal to distal segments, but to our knowledge only a single study has reported segment-specific expression of claudins in fishes [*Danio rerio* (64)].

Several aspects of teleost kidney functional anatomy have been investigated since Hickman and Trump's (41) extensive survey. In contrast to mammals, vascular responses may be quite significant during osmotic adjustments and may overall

contribute to the large change in net urine output upon acclimation to SW (15). On the other hand, deep insight into segment-specific expression and regulation of solute- and water-transporting proteins and tight junction proteins in response to osmotic adjustments is lacking. Tubular localization of selected ion and solute transporters and tight junction proteins have been established by in situ hybridization and immunohistochemistry in a few species (28, 49, 50). Renal gene expression analyses have, however, typically used whole kidney homogenates (e.g., Refs. 11 and 56) and do not provide segment-specific information.

Our goal was to provide segment-specific information about transcript levels of several transport proteins in the Atlantic salmon kidney in relation to environmental salinity. We used advanced laser capture microdissection (LCM) (30) to isolate enriched cell material from renal proximal and distal tubules of Atlantic salmon acclimated to either FW or SW and subsequently analyzed by quantitative PCR (qPCR) the mRNA expression profiles of a list of well-described transport proteins (see Table 1). The list of genes comprised four categories known from previous studies (listed in brackets) to be expressed in teleost kidneys: aquaporins [5 family members (27, 28, 84)], tight junction proteins [12 claudins (52, 82, 85) and occludin (19)], solute transporters [13 ion pumps and channels (3, 10, 16, 21, 23, 33, 45–47, 49, 50, 66)] and FXD proteins [2 family members (81)], which are potential modulators of NKA activity (36). Some of the targets have been reported previously in kidneys of different teleosts but never in a comprehensive analysis in one species and with focus on segmental mRNA regulation in response to osmotic environment.

## MATERIALS AND METHODS

### *Fish and Maintenance*

Juvenile Atlantic salmon (*Salmo salar*, size range 19–23 cm) were obtained from the Danish Center for Wild Salmon (Randers, Denmark). Fish were acclimated to mechanically and biofiltered recirculating municipal freshwater (FW) and kept on a simulated natural light cycle. Fish were fed 0.5% body weight<sup>-1</sup> three times a week with commercial trout pellets (Ecolife, Biomar, Aarhus, Denmark). All experimental procedures were approved by the Danish Animal Experiments Inspectorate in accordance with the European convention for the protection of vertebrate animals used for experiments and other scientific purposes (no. 86/609/EØF).

### *Kidney Sampling*

Six salmon were transferred to a 400-liter tank with 24 ppt recirculated artificial sea water (SW; Red Sea Salt, Eliat, Israel) and allowed to acclimate for 3 days before bringing the salinity up to 28 ppt and acclimated for 7 days before sampling. In parallel, six fish were sham transferred to FW. Upon sampling, fish were quickly stunned and euthanized by cervical dislocation and brain pithing. The entire kidney was carefully dissected out and orientation maintained to ensure uniform sampling for each specimen. Blocks (3–4 mm) of kidney tissue were cut transversally, placed in Optimum Cutting Temperature medium (Thermo Fisher, Waltham, MA), quickly frozen on dry ice, and subsequently stored at  $-80^{\circ}C$ .

### *Staining, Fixation, and LCM*

Tissue blocks were transferred to a cryotome before cutting and allowed to acclimate to the set temperature for 30 min. Sections were cut at 20  $\mu m$  and transferred to an RNase-free LCM slide (Molecular

Table 1. Primer sequences and NCBI accession numbers for the targets analyzed in Atlantic salmon proximal and distal tubules

Category	Target	Forward Sequence	Reverse Sequence	Amplicon Size	NCBI Accession No.	
Ion transporters	<i>nka-α1a</i>	CCCAGGATCACTCAATGTCAC	TCAAAGGCCAAATGAGTTTAAAT	90	XM014209857	
	<i>nka-α1b</i>	TGCTACATCTCAACCAACAACATT	CACCATCACAGTGTTCATTGGAT	80	XM014152156	
	<i>nkcc1a</i>	TCCATCGACATGAAGGAC	CGTTCATCATCGTTCACCT	104	NM001123683	
	<i>nkcc2</i>	GTCCGTCGGTGGTCAGTG	GCTCACACTCCCAGCGTT	86	NM001141520	
	<i>ncc</i>	GTCCGAACTTCCACCAAAA	TTCTACTGGCAGTGTCCAAG	139	XM014124221	
	<i>nhe3</i>	AGAGCAGCCGTGACAGAACT	AGCAATACCAACCCACTCTC	155	XM014166803	
	<i>cftr</i>	CCTTCTCCAATATGGTTGAAGAGGCAAG	GAGGCACTTGGATGAGTCAGCAG	84	AF319595	
	<i>clc-kb</i>	GCCCTATCAGTGGTGTGTT	AGAGCAGATGGAAGGTGAGC	118	XM014135359	
	<i>sglt1</i>	GGAACAGCACAGAGGAGAGG	GGCTCTCAATATCCACAAAAG	89	GU129697	
	<i>sglt2</i>	GATGAGGTGGGTGTGTGTT	CAGTTTGGGGTAGGCGATGT	87	NM001140069	
	<i>slc26a6C</i>	CCTACCTGTCCGAGCCACTG	TTGGAGCACACCTCCACCAG	151	XM021568872	
	<i>scl41a</i>	CAATGTGAACTCTCGTTCGGC	GTGCTGTGTCTCCCTGCAT	102	XM014132936	
	<i>cnm3</i>	CTCATACGGGTGACTCGCAT	AGCTTGGTCTGACTGTGGG	110	XM014128009	
	FXyD	<i>fyxd2</i>	ATGGGTGGAGAAACATCACA	AGCAATACCCAGGCAGAAGA	114	BK006252
		<i>fyxd12a</i>	GCTCCTGAGTACGACCCCTGA	ATCATGATGACCGCAACAAA	89	BK006249
	Tight junction proteins	<i>cldn3a</i>	AGGGTTGGAGTTAGTGGGGA	TGACGATGTGCTGCCGATA	113	XM014162769
		<i>cldn3b</i>	ATCCTGTGCTGTAGTTGCC	CTTTTGTATAGCCCGCTGGG	110	XM014162770
<i>cldn3c</i>		TCGGAGCCAAGTGTACCAAC	CAAAGGAAAACGGGGATGAG	117	BK006383	
<i>cldn7</i>		GCCTTCCAGTGTGAGACCTAC	AAAAGACCACGGAGACCACC	91	XM014195723	
<i>cldn8</i>		TGTGGCTGGGGTATACTGC	CAGGCTGGTAGTTCCTCC	116	XM014163650	
<i>cldn10b</i>		ACGGCACAGTTATCACCACA	GGAAAGTCCTTGCAAGTTGGA	94	XM014165558	
<i>cldn10e</i>		ATCAAGGTGGCCTGGTACTG	GACCAGACACAGGGAAGTC	95	XM014150521	
<i>cldn12</i>		GTTCTGGGCGGTGCTATC	GACTGTGAGAAAGTGCCTGT	94	XM014202033	
<i>cldn15a</i>		GGCACGCTGTGAGAAACAACA	TAGGAAGTGGCAGCCTGACT	92	XM014206890	
<i>cldn28a</i>		TGACTGCTCAGGTCATCTGG	GGTAAGGCCAGAAGGGAGTC	100	BK006401	
<i>cldn28b</i>		TTCTACCAGGGCTCCATCAG	ATGGGCAGAGCACAGATGAT	107	BK006402	
<i>cldn30c</i>		TGATCATTGGAGAGGGTTC	AACATAGTCCCTGGGTGCTG	104	BK006405	
<i>occln</i>		GACAGTGAGTTCGCCACCAT	ATCTCTCCCTGCAGGTCCCT	101	XM014137436	
Aquaporins	<i>aqp1a</i>	CTACCTTCCAGTGGTCCCTG	TGATACCCGAGCCTGTGTGT	141	BT046625	
	<i>aqp1ab</i>	CTGTGGGTCTGGGACATCTT	TAAGGGCTGCTGTACACCT	153	BT045044	
	<i>aqp3a1</i>	TGACAGGAAGAGCCAGGAG	GAGGCTGAGCTTAGGGGTA	187	XM014160893	
	<i>aqp8bb1</i>	GACACGCCCTGCTCATTCCG	GTCTCCACCACCATTCAACAA	71	BT059566	
	<i>aqp10b1</i>	GGTGTGGTGATCGGAGTCT	CGCCCTAAACACCTCATCC	121	XM014142217	
Norm genes	<i>18s rRNA</i>	TCTCGATTCTGTGGGTGGT	CTCAATCTCGTGTGGCTGA	170	AJ427629	
	<i>β-actin</i>	TGGGACGACATGGAGAAGAT	AGAGGCGGTACAGGGACAACA	201	KU885449	
	<i>ef1α</i>	GAGAACCATTGAGAAGTTCGAGAA	GCACCCAGGCATACCTGAAAG	71	AF321836	

NCBI, National Center for Biotechnology Information.

Machines, Eching, Germany). They were allowed to air dry at room temperature for 1 min and then placed in 70% ethanol with RNase inhibitor (1:500) for 1 min (ProtectRNA RNase Inhibitor 500× Concentrate, Sigma-Aldrich St. Louis, MO). The slide was gently dried around the sections with a tissue and to distinguish proximal and distal tubules 25 μL BCIP/NBT Liquid Substrate System (Sigma-Aldrich) was pipetted directly onto the sample and incubated for 2 min at room temperature. The brush border of proximal tubules has alkaline phosphatase activity (62), which may be visualized by reacting with the BCIP/NBT substrate (Fig. 1). Subsequently, color development was terminated by placing in di-ethyl-pyrocyanide (DEPC)-treated water for 30 s. Proximal tubules were thus identified by the presence of a colored brush border. Distal segments were recognized as being BCIP/NBT negative by having cuboidal cells and generally exhibiting smaller lumen diameter than proximal tubules. They were further distinguished from collecting ducts, which also lack the brush border but have larger diameter than distal tubules and are surrounded by layers of smooth muscle and connective tissue (5).

The slide was gently dried around the sample, and Mayer's hematoxylin (Sigma-Aldrich) was applied directly to the slide and it was incubated for 1 min before being placed in DEPC-treated water for two times for 30 s. Excess moisture on the slide was wiped away before being placed in 70% ethanol with RNase inhibitor for 30 s and then moved to 70% ethanol for 30 s. Finally, the slide was allowed to air dry for 2 min. All ethanol dilutions were prepared using DEPC-treated water. The slide was quickly moved to the laser microscope (SmartCut, Olympus, Tokyo, Japan), and ~200 cross sections of either

proximal or distal tubules were dissected from the slide within 10 min (Fig. 1) and collected in separate isolation caps (with diffuser, Molecular Machines). Two slides were dissected from each of six fish per salinity. After sample collection, 100 μL TRI Reagent (Sigma-Aldrich) were added to the sample and kept at 4°C for extraction and storage. All downstream treatments and analyses were performed on the individual samples, and subsequently the data were averaged for each fish, giving an *n* value of 6 for the transcript analyses.

#### RNA Isolation, cDNA Synthesis, and qPCR

Cells were lysed by manual pipetting and vortex mixing. Total RNA was isolated following the manufacturer's protocol and adapted for the volume of TRI reagent used. RNA pellets were dissolved by manual pipetting in a total of 10 μL of DEPC-treated water. RNA samples were then treated with water-saturated butanol to remove potential phenol contamination (55). Excess butanol was removed with water-saturated diethyl ether. The final RNA concentration was analyzed on an Agilent Bioanalyzer (Santa Clara, CA), and the total yield was typically around 12 ng. cDNA synthesis was performed using SuperScript IV VILO Master Mix (Thermo Fisher Scientific, Waltham, MA) following the manufacturer's protocol.

mRNA sequences for Atlantic salmon target transcripts were identified in the National Center for Biotechnology Information (NCBI; Bethesda, MD) GenBank (<https://www.ncbi.nlm.nih.gov/>) and used to design specific primers to analyze the following targets: *nkcc2*, *ncc*, *cftr*, *clc-k*, *sglt1*, *sglt2*, *scl41a1*, *slc26a6C*, *cnm3*, *cldn3a*, *cldn3b*,

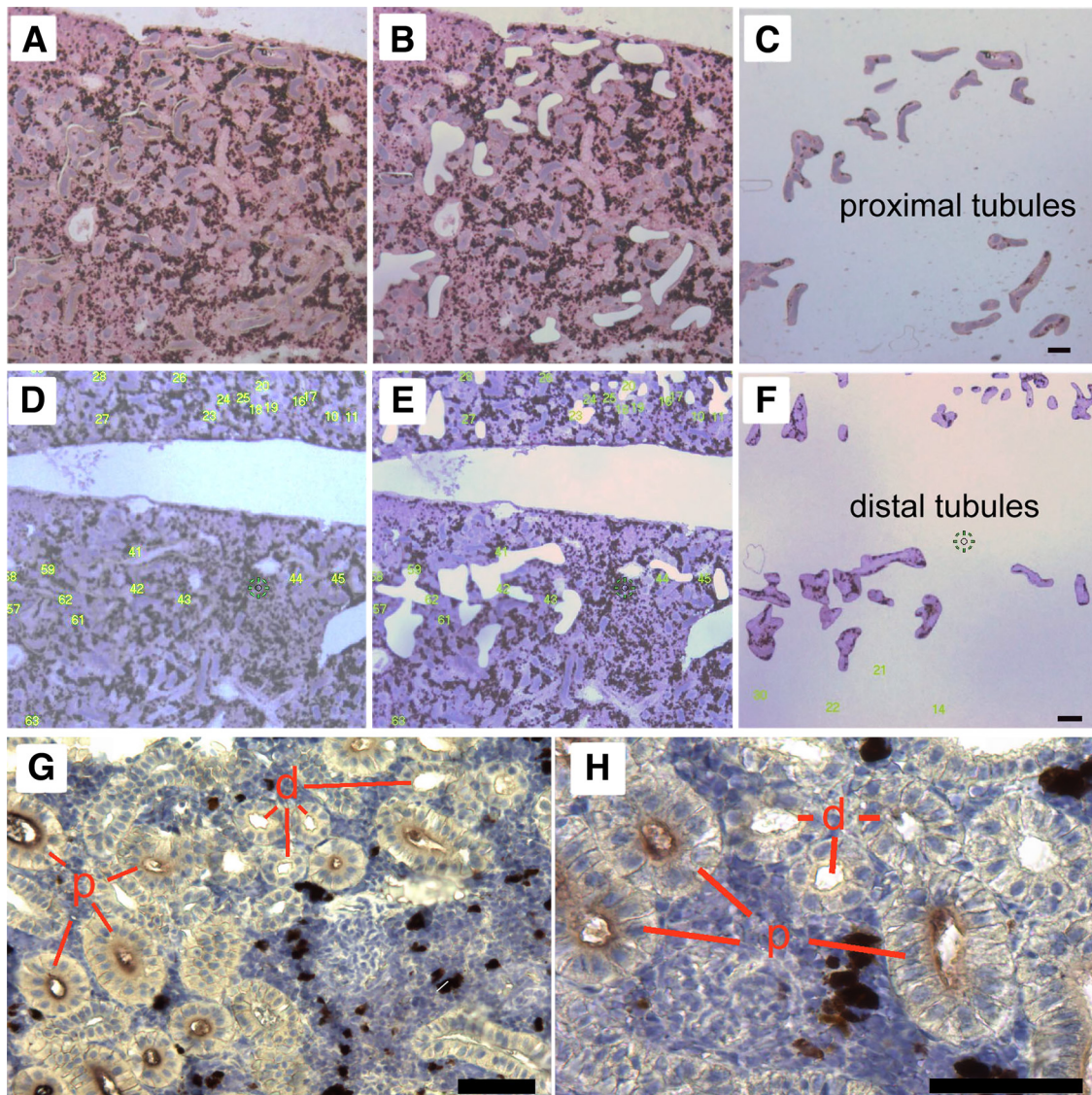


Fig. 1. A–F: images showing 20- $\mu\text{m}$  cryosections before (A and D) and after (B and E) laser-capture microdissection of Atlantic salmon kidney tubule cross-sections. C and F: dissected proximal and distal tubule sections, respectively, collected on isolation caps. The sections are stained with BCIP/NBT and viewed through the isolation cap. In cryosections, BCIP/NBT stains the brush border of proximal tubules light blue. G and H: 5- $\mu\text{m}$  paraffin-embedded kidney sections stained with Mayer's hematoxylin (blue: nuclei) and BCIP/NBT (brush border appears purple-brownish in paraffin sections), showing the distinction between proximal (p) and distal (d) tubules based on the presence or absence, respectively, of brush border staining. A–F:  $\times 50$ ; G:  $\times 200$ ; H:  $\times 400$  magnification. Bars = 100  $\mu\text{m}$  (A–F) or 50  $\mu\text{m}$  (G and H).

*cldn3c*, *cldn7*, *cldn8*, *cldn10b*, *cldn12*, *cldn15a*, *ocln*, *18s rRNA*, and  $\beta$ -actin. Primers were generated using Primer3 software [http://www.bioinfo.ut.ee/primer3-0.4.0/primer3/ (52)] and synthesized by ThermoFisher Scientific. The following primers have been published previously: *ef1 $\alpha$* , *aqp1aa*, *aqp1ab*, *aqp10b1* (84); *aqp3a1* (28); *aqp8bb1* (26); *cldn10e*, *cldn28a*, *cldn28b*, *cldn30c* (82); *fxyd2*, *fxyd12* (81); *nka- $\alpha$ 1a*, *nka- $\alpha$ 1b* (58), *nkcc1a* (83), and *nhe3* (47). Primer sequences and accession numbers are listed in Table 1. Elongation factor 1- $\alpha$  (*ef1 $\alpha$* ),  $\beta$ -actin ( *$\beta$ -actin*), and 18s ribosomal RNA (*18s rRNA*) were used as normalization genes (7).

qPCR was performed in a final volume of 15  $\mu\text{L}$  with a 200-nM primer concentration and run on a Bio-Rad CFX96 platform thermocycler (Bio-Rad, Hercules, CA) using RealQ Plus 2 $\times$  Master Mix (Ampliqon, Odense, Denmark). After an initial heating to 95°C for 15 min, the majority of targets were analyzed using a two-step qPCR protocol (40 cycles of 95°C/15 s 60°C/1 min) followed by melt curve analysis from 60 to 95°C with a gradient of 5 s per 0.5°C to confirm

reaction specificity. The following targets were analyzed using a three-step protocol {95°C/15 s, annealing temperature ([ $T_{\text{ann}}$ ])/15 s, 72°C/30–45 s;  $T_{\text{ann}}$  in brackets}: *aqp10b* [60], *nkcc1a* [60], *nkcc2* [58,9], *nhe3* [60], *clc-k* [59], *slc41a1* [59], *slc26a6* [60], *cnmm3* [59,8], *sglt2* [60], *cldn3a* [61], *cldn3b* [60], *cldn3c* [60], *cldn7* [63], *cldn15a* [69], *ocln* [60], and  $\beta$ -actin [60]. The amplification efficiency  $E_a$  was determined for each primer set. For each gene, the relative mRNA level was calculated as  $C_n = (1 + E_a)^{-C_t}$ , where  $C_t$  is the threshold cycle of the target gene and  $E_a$  is the amplification efficiency (69). This number was then normalized to the geometric mean of the relative mRNA level of the three normalization genes. There was no significant variation in the geometric mean (see Fig. 8F). No template controls (NTCs) were included in all qPCR runs to confirm template specificity and to ensure there were no primer-dimers present. Amplicon sizes were routinely checked by 2.5% agarose gel electrophoresis. No amplification controls (NACs) were run to assure that

genomic DNA contamination was negligible (always less than  $2^{-8}$  of the target gene level).

### Immunohistochemistry

Kidney tissue dissected from FW-acclimated Atlantic salmon was used for immunohistochemistry of the sodium-glucose cotransporter-1 (SGLT-1) and the NKA  $\alpha$ -subunit. These targets were chosen to verify accordance between segmental protein and mRNA expression. Tissue was fixed overnight 4°C in 4% phosphate-buffered paraformaldehyde and then rinsed and stored in 70% ethanol. Dehydration, embedding, sectioning, and immunostaining followed the protocol published in Ellis et al. (25). The sections were incubated with a cocktail of polyclonal rabbit antiserum against mouse SGLT-1 (1:500; catalog no. 07-1417, Sigma-Aldrich) in combination with a mouse monoclonal antibody against the  $\alpha$ -subunit of NKA ( $\alpha 5$ ; 1:1,000; The Developmental Studies Hybridoma Bank developed under the auspices of the National Institute of Child Health Development and maintained by the University of Iowa, Department of Biological Sciences, Iowa City, IA). The epitope of the SGLT-1 antibody corresponds to a 19 amino acid sequence (402–420: STLFTMDIYTKIRKKASEK) of the putative extracellular loop of mouse SGLT-1. A blast search in GenBank [National Center for Biotechnology Information (NCBI), Bethesda, MD; <https://blast.ncbi.nlm.nih.gov/Blast.cgi>] revealed that this epitope shares 17/19 and 12/19 identity with the Atlantic salmon Sgl1 and Sgl2 sequences, respectively (Accession Nos. ADB13172 and NP001133541). The antiserum reveals a single 70-kDa band in Western blots using a PC3 lysate (Sigma-Aldrich). Another study (70) showed strong brush border staining in trout intestine using this antiserum, and we have verified a similar brush border staining in the Atlantic salmon intestine (Supplemental Fig. S2; all Supplemental Material is available at <https://doi.org/10.6084/m9.figshare.11733906.v1>). After primary incubation, sections were incubated with goat anti-rabbit IgG Alexa Fluor 568 and goat anti-mouse IgG Oregon green 488 (1:1,000, Invitrogen, Carlsbad, CA) for 1 h at 37°C. Nuclei were counterstained with 4',6-diamidino-2-phenylindole (DAPI, 0.1  $\mu$ g/mL in PBS) for 10 min. Sections were finally washed four times for 5 min in PBS, and coverslips were mounted using ProLong Gold antifade (Invitrogen). Negative controls in the absence of primary antibody/antiserum were completely blank (not shown).

### Statistical Analysis

All statistical analyses were performed with GraphPad Prism 8.0 software (San Diego, CA). The Brown-Forsythe test was used to confirm homogeneity of variances to meet the assumptions of the ANOVA, and the data were log transformed when required. A two-way ANOVA was used to analyze the expression data, followed by pairwise comparisons with Holm-Sidak's multiple comparison test if a significant interaction occurred. In the few cases where homogeneity of variance could not be obtained, data were analyzed by a Welch ANOVA (*aqp8bb1*, *cldn8*, *cldn28a*, and *cldn30c*). Results are expressed as means  $\pm$  SE of the mean being statistically different when  $P < 0.05$ .

## RESULTS

### Histology and Immunohistochemistry

Distinct identification of proximal (P) kidney tubules is shown in Fig. 1, A–C, G, and H with the presence of BCIP/NBT staining of the brush border of the inner lining of tubules due to the presence of alkaline phosphatase reactivity. For unknown reasons the staining appeared bluish in cryosections and purple-brownish in paraffin sections. Immunofluorescent staining of the NKA  $\alpha$ -subunit (Fig. 2) showed weak lateral and basolateral staining of P tubule cells and a much more

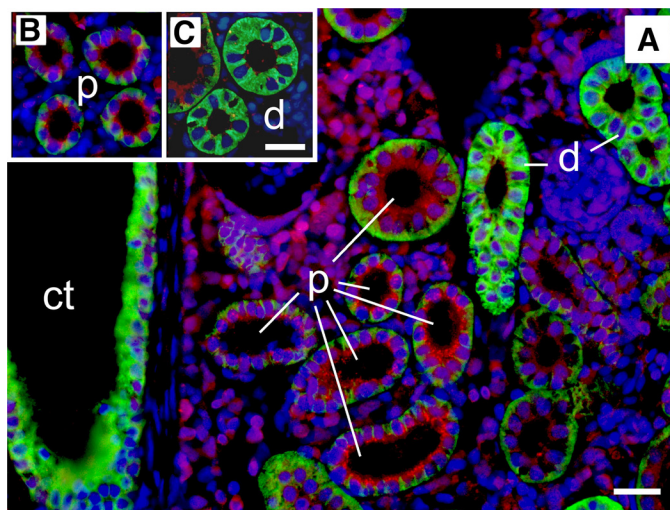


Fig. 2. A: 5- $\mu$ m-thick paraffin sections of Atlantic salmon kidney coimmunostained with antibodies against the  $\text{Na}^+\text{-K}^+\text{-ATPase}$   $\alpha$ -subunit (NKA; Alexa Fluor Oregon green) and the sodium-glucose cotransporter-1 (SGLT1, Alexa Fluor 568, red). Sections were counterstained with DAPI (blue) for visualization of nuclei. Based on the staining pattern of NKA, tubule segments are identified as being proximal (p; basolateral weak staining), distal (d; intense staining throughout the cell), or collecting tubules (ct; intense staining, large tubule diameter). B and C: proximal and distal tubules, respectively, from another section at  $\times 200$  magnification. Bars = 20  $\mu$ m.

intense staining and dispersed distribution in cells of the distal (D) tubules. An intense Sgl1 immunoreactivity was seen at the apical brush-border zone of P tubules and a low ubiquitous dispersion in cells of other tubule types.

### Tubular Gene Expression in FW and SW

Several of the investigated targets show segmental differences and/or salinity-induced differences. A summary of the expression statistics is shown in Fig. 3.

*Na<sup>+</sup> and Cl<sup>-</sup> transporters.* *nka- $\alpha$ 1a* is generally expressed at very low levels compared with the *nka- $\alpha$ 1b* isoform. Both isoforms are expressed at higher levels in D tubules, especially the *nka- $\alpha$ 1b* isoform, with no effect of salinity (Fig. 4A and 4B, respectively). The secretory *nkcc1a* is generally expressed at low levels being highest in D tubules and unresponsive to salinity (Fig. 4C). The absorptive *nkcc2* isoform is also at its highest levels in D tubules (Fig. 4D). There is a significant interaction between segment and salinity and an inhibitory effect of SW in the P tubules (Fig. 4D). *ncc* is predominantly expressed in D tubules, and there is a significant interaction between segment and salinity and an overall stimulatory effect of SW (Fig. 4E). *nhe3* is expressed at higher levels in P tubules and increases significantly in SW (Fig. 4F). *cfr* is expressed at similar levels in P and D tubules and increases in SW by 1.7- and 2.4-fold in P and D tubules, respectively (Fig. 4G). *clc-k* is predominantly expressed in the D tubules with no effect of salinity (Fig. 4H). *slc26a6C* is expressed at greater than threefold higher levels in D compared with P tubules, with a significant decrease in P tubules in SW. *sgl1* is almost exclusively expressed in P tubules and with an overall stimulatory effect of SW in both segments (Table 2) being most pronounced in the P tubules. This is in contrast to *sgl2*, which is expressed in both P and D tubules, although at two- to sixfold higher levels in D tubules (Table 2).

Protein category	Target	Localization	Salinity	Interaction
Ion transport proteins	<i>nka-α1a</i>			
	<i>nka-α1b</i>			
	<i>nkcc1</i>			
	<i>nkcc2</i>			
	<i>ncc</i>			
	<i>nhe3</i>			
	<i>cftr</i>			
	<i>clc-k</i>			
	<i>slc26a6C</i>			
	<i>slc41a1</i>			
	<i>cnnm3</i>			
	<i>sglt1</i>			
	<i>sglt2</i>			
FXYP proteins	<i>fxyd2</i>			
	<i>fxyd12a</i>			
Tight junction proteins	<i>cldn3a</i>			
	<i>cldn3b</i>			
	<i>cldn3c</i>			
	<i>cldn7</i>			
	<i>cldn8</i>			
	<i>cldn10b</i>			
	<i>cldn10e</i>			
	<i>cldn12</i>			
	<i>cldn15a</i>			
	<i>cldn28a</i>			
	<i>cldn28b</i>			
	<i>cldn30c</i>			
	<i>occln</i>			
Aquaporins	<i>aqp1aa</i>			
	<i>aqp1ab</i>			
	<i>aqp3a1</i>			
	<i>aqp8bb1</i>			
	<i>aqp10b1</i>			

Fig. 3. Statistical summary of the target genes analyzed in Atlantic salmon proximal and distal kidney tubules showing their predominant segmental localization, factorial response to salinity and statistical interaction between segment and salinity. Based on the statistical analysis of each target gene, the following color key is assigned for statistical differences: 1) light green: proximal > distal; dark green: distal > proximal; no color: proximal = distal; 2) light blue: freshwater (FW) > seawater (SW); dark blue: SW > FW; no color: FW = SW; and 3) gray: interaction between segment and salinity; no color: no interaction.

*Mg<sup>2+</sup> transporters.* Transcript levels of *slc41a1* and *cnnm3* are much higher in P than D tubules, and *slc41a1* is stimulated sixfold by salinity (Fig. 5, A and B).

*fxyd proteins.* *fxyd2* displays significantly higher expression in the D tubule segment, with an overall inhibitory effect of SW (Fig. 6A). Expression of *fxyd12a* is markedly higher in P tubules with an overall stimulatory effect of SW (Fig. 6B).

*Tight junction proteins.* Most of the claudin transcripts investigated are at similar levels in the P and D tubules (Fig. 7). An exception to this is *cldn3b*, *cldn12*, and *cldn15a*, which are at higher levels in the P than in the D tubules (Fig. 7, B, H, and I). *cldn15a* is at ca. 50-fold higher levels in P than in D tubules. *cldn3a* (Fig. 7A) and *occln* (Table 2) are expressed at a threefold higher level in the D compared with P tubules. Five out of the 12 claudins are affected by salinity: *cldn3a*, *cldn3b*, *cldn10b*, *cldn10e*, and *cldn28a* are overall expressed at higher levels in SW compared with FW (Fig. 7, A, B, F, G, and J).

*Aquaporins.* *aqp1aa* is overall expressed at higher levels in D compared with P tubules. There is a significant interaction between segment and salinity with a 30-fold higher expression in the D tubules of SW-acclimated salmon (Fig. 8A). *aqp1ab* expression is significantly higher in D compared with P tubules and shows a decreased expression in both tubule types in SW (Fig. 7B). *aqp3a1* is evenly expressed in P and D tubules and is significantly upregulated in SW compared with FW (Fig. 8C). *aqp8bb1* is expressed at higher levels in P tubules and unresponsive to salinity (Fig. 8D). *aqp10b1* is severalfold higher in P compared with D tubules, especially in SW with a 2.5-fold increase in the P tubules (Fig. 8E).

## DISCUSSION

### Validation of the Microdissection Technique

This study is the first to apply the LCM technique to analyze gene expression separately in proximal and distal kidney tubules of any teleost. Assuming that cell types are properly identified, LCM furthers analysis of “clean” tissue transcript profiles without contamination from, e.g., blood cells. BCIP/NBT brush-border staining was used as an identification tool to distinguish proximal (P) from distal (D) tubule segments (Fig. 1). This is based on our knowledge that PI and PII segments possess a distinct luminal brush border with distinct alkaline phosphatase activity, whereas distal tubules do not (5, 48, 50). Other studies have used periodic acid-Schiff staining to facilitate the same distinction (50, 80). The brush border is more intense in PI segments compared with PII segments in rainbow trout (5), but our methodology did not allow for such discrepancy. Thus the present proximal sample represents both proximal regions. The distinction method is supported by the expression pattern of NKA, which is located basolaterally at relatively low intensity in P tubules and in deep basolateral membrane infoldings at much higher intensity in distal D tubules (Fig. 2) (49, 50, 80). Furthermore, the localization patterns of Sglt1 protein in P tubules and NKA predominantly in D tubule cells (Fig. 2) were in full agreement with their transcripts being primarily expressed in these same segments (Table 2 and Fig. 4, A and B, respectively).

Vascular effects are important in the regulation of kidney function in euryhaline teleosts and may contribute more to regulation than tubular effects (28). Glomerular filtration rate (GFR) is considerably reduced in SW compared with FW teleosts (14, 24, 63), which is mostly achieved by a marked reduction in the number of actively filtering glomeruli. At the same time, actively filtering individual nephrons may exhibit almost three times higher filtration rate in SW- than in FW-acclimated *O. mykiss* (14, 15). This underlines that the kidney makes a significant switch from being filtratory in FW to being predominantly secretory in SW. We investigated mRNA expression of an extensive range of ion and solute transporters, claudins, and aquaporins with the aim to gain deeper insight into tubular localization patterns and particularly the tubular regulation of these targets in relation to environmental salinity. Previous studies have localized some of the selected protein targets [e.g., NKA (50), NKCC2 (49), CIC-K (66), occludin (19), Aqp8bb1 (28)] in various teleosts [e.g., rainbow trout, killifish, mefugu, goldfish (*Carassius auratus*)], but the larger picture of segmental mRNA expression and especially quanti-

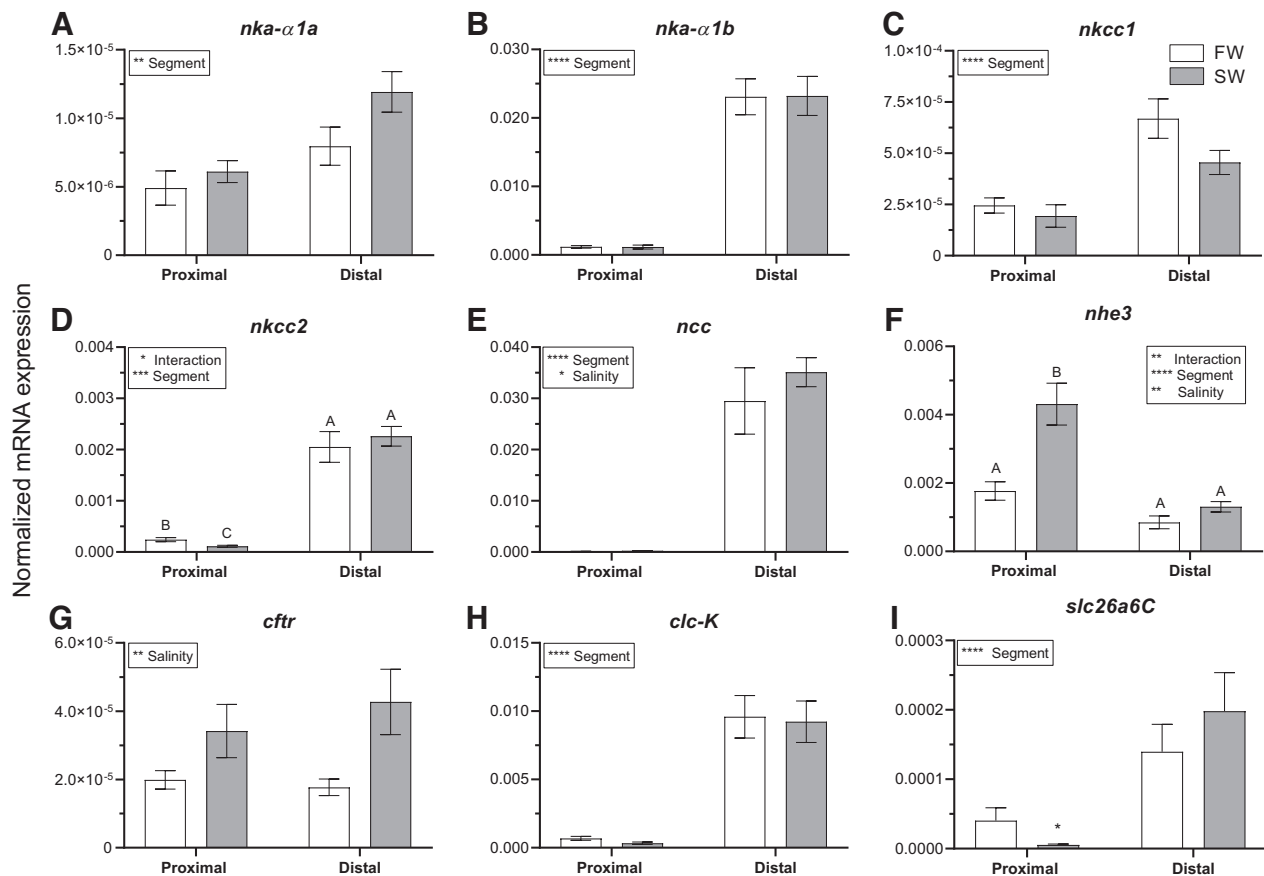


Fig. 4. Normalized mRNA levels of  $\text{Na}^+$ - and  $\text{Cl}^-$ -transporting genes expressed in proximal and distal tubules microdissected from kidneys of Atlantic salmon acclimated to freshwater (FW) (white bars) or seawater (SW) (gray bars). A: *nka- $\alpha$ 1a*; B: *nka- $\alpha$ 1b*; C: *nkcc1*; D: *nkcc2*; E: *ncc*; F: *nhe3*; G: *cftr*; H: *clc-K*; I: *slc26a6C*. Inset: explanations of overall factorial effects (two-way ANOVA). In case of significant factorial interaction, post hoc multiple comparisons were made with Holm-Sidak's test. Data are means  $\pm$  SE ( $n = 6$ ). Bars sharing letters are not significantly different. \* $P < 0.05$ , \*\* $P < 0.01$ , \*\*\* $P < 0.001$ , \*\*\*\* $P < 0.0001$ .

tative responses to salinity has not been described comprehensively in any teleost.

#### Solute Transport in Tubular Segments

Urine production in glomerular kidneys is based on filtration of the blood followed by subsequent modification through most

Table 2. Normalized transcript abundance of *sglt1*, *sglt2*, and *ocln* in proximal and distal tubules of *Salmo salar* acclimated to FW or SW

Target/Salinity	Tubule Segment		Statistics
	Proximal	Distal	
<i>sglt1</i> <sup>a,b</sup>			
FW	0.0054 (0.00041)	0.00021 (0.000040)	P > D
SW	0.0105 (0.0034)	0.00034 (0.000034)	SW > FW
<i>sglt2</i> <sup>a</sup>			
FW	0.00034 (0.00012)	0.0010 (0.00022)	D > P
SW	0.00017 (0.000036)	0.0011 (0.00025)	
<i>ocln</i> <sup>a</sup>			
FW	0.0000039 (0.0000009)	0.000012 (0.0000015)	D > P
SW	0.0000024 (0.0000006)	0.000011 (0.0000007)	

Values are means (SE);  $n = 6$ . Transcript abundance was normalized to the geometric mean of 3 reference genes. Statistics are summarized in the "Statistics" column. D, distal; P, proximal; FW, freshwater; SW, seawater. <sup>a</sup>Overall effect of "tubule segment" (two-way ANOVA,  $P < 0.001$ ); <sup>b</sup>overall effect of "salinity" (two-way ANOVA,  $P < 0.01$ ).

of the nephron. The fractional reabsorption of water is variable depending on, e.g., species and salinity, typically in the range 25–50% (41), and reabsorption occurs in both P and D segments and continues in the bladder of SW teleosts (59). Nonetheless, tubular fluid secretion may also occur in P segments and is an ancient and well-conserved function of this segment throughout the vertebrate lineage (8). Since fluid transport is generally linked to solute transport, reabsorption as well as secretion of solutes is expected to occur in subregions of the P segments. For example, our data support that there are simultaneous reabsorption and secretion of  $\text{Na}^+$  taking place in the P segment. Glucose (and  $\text{Na}^+$ ) is reabsorbed proximally via apical SglT proteins irrespective of salinity. There is kinetic evidence of  $\text{Na}^+$ /glucose (1:1) cotransport in the trout kidney (16, 33), and by using highly isoform-specific primers, our data show a strong expression of *sglt1* almost exclusively in P tubules, which was supported by apical brush border localization of SglT1 protein predominantly in P tubules. On the other hand, *sglt2* is expressed in both tubule segments with elevated transcript levels in the D tubules. This is at variance with mammals, where SGLT2 is expressed in early proximal segments and SGLT1 exclusively in later proximal convoluted tubules to optimize glucose reabsorption. Interestingly, the *sglt1* mRNA level was significantly higher in SW kidney, which suggests higher capacity for resorption of glucose (and  $\text{Na}^+$ ) in the hyperosmotic environment. Renal SglT expression

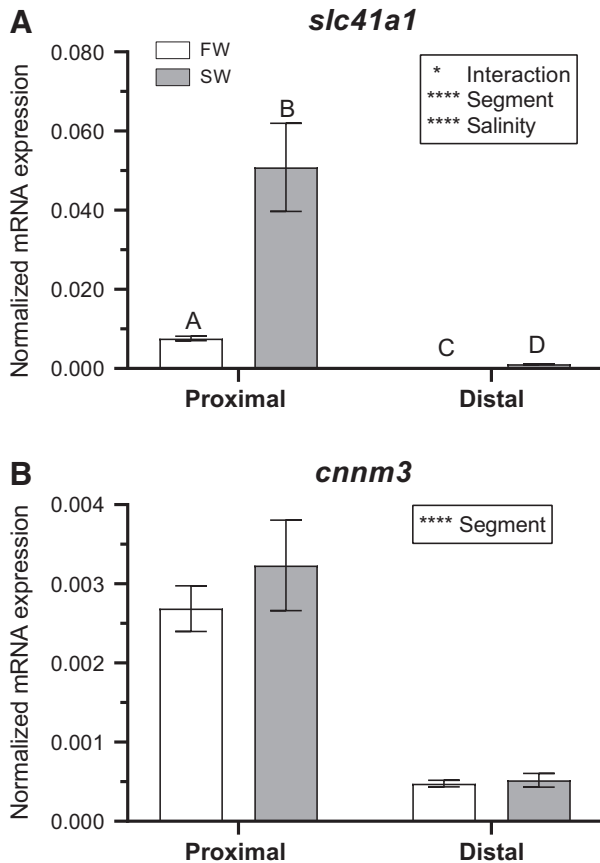


Fig. 5. Normalized mRNA levels of  $Mg^{2+}$ -transporting genes expressed in proximal and distal tubules microdissected from kidneys of Atlantic salmon acclimated to freshwater (FW) (white bars) or seawater (SW) (gray bars). A: *slc41a1*; B: *cnnm3*. Inset: explanations of overall factorial effects (two-way ANOVA). In case of significant factorial interaction, post hoc multiple comparisons were made with Holm-Sidak's test. Data are means  $\pm$  SE ( $n = 6$ ). Bars sharing letters are not significantly different. \* $P < 0.05$ , \*\*\*\* $P < 0.0001$ .

has not previously been analyzed in any teleost; yet, Sglt1 and -2 isoforms have been demonstrated in proximal, distal, and collecting tubules of the elasmobranchs *Squalus acanthias* (2) and *Leucoraja erinacea* (3). Further studies of the two isoforms are needed to further clarify reabsorption kinetics.

The majority of proximal  $Na^+$  reabsorption is mediated apically by other transporters (16) such as the apical  $Na^+/H^+$  exchanger [*nhe3* (47)], which doubles expression in SW. On the other hand, the involvement of apical *nkcc2* and *ncc* is questionable in the P segment, since both are expressed at very low levels. This agrees with the situation in euryhaline puff-fishes (49), killifish, and rainbow trout (50), where they are located exclusively in the D segment.  $Na^+$  reabsorption is followed by apical  $Cl^-$  reabsorption, likely to occur via a Slc26a6 protein. Kato et al. (48) demonstrated that a Slc26a6A paralog was the predominant paralog expressed in the P tubules in mefugu and was 30-fold elevated after SW acclimation. In *S. salar*, this protein is expressed in at least two paralogs [*Slc26a6A*-like (12); *Slc26a6C*-like (37)]. We analyzed both paralogs using specific primers and found that the *Slc26a6A* paralog is generally expressed at very low levels in all renal tubules (Ct values  $> 35$ , not shown). The *Slc26a6C* paralog is expressed at much higher levels (Ct values 26–33, Fig. 4I) and

at a significantly higher level distally. Curiously, the transcript level declined in P tubules upon SW acclimation. Genz et al. (38) reported similar expression of this paralog in whole kidney of rainbow trout (*O. mykiss*) in FW and SW. Kato et al. (48) proposed that the mefugu Slc26a6A (and -B) paralog may handle both  $Cl^-/HCO_3^-$  and  $Cl^-/SO_4^{2-}$  exchange, whereas the -6C paralog showed no signs of this function when expressed in *Xenopus* oocytes. The functional properties of these paralogs are presently unknown in salmon.

In the P segment, there is also capacity to secrete  $Na^+$  as evidenced by the presence of the secretory *nkcc1a* isoform, which is unaffected by salinity. The present study does not reveal whether absorption and secretion take place in the same or in different cell types in the P segment. Katoh et al. (50) reported basolateral NKCC activity in P tubules of killifish but not in trout. In addition to the NKCC1 cotransporter, the secretory pathway for NaCl most likely involves an apical CFTR-chloride channel and a paracellular  $Na^+$ -leak pathway. The former is supported by the presence of a *cfr* transcript that is stimulated 1.7-fold by salinity, suggesting an increased capacity for  $Cl^-$  secretion in SW. The CFTR is expressed throughout most of the mammalian nephron where its role is debated (78), and to our knowledge *cfr* expression in fish kidneys has only been documented during a short period of European sea bass, *Dicentrarchus labrax*, ontogeny (13). Our data thus support the observation of Cliff and Beyenbach (20)

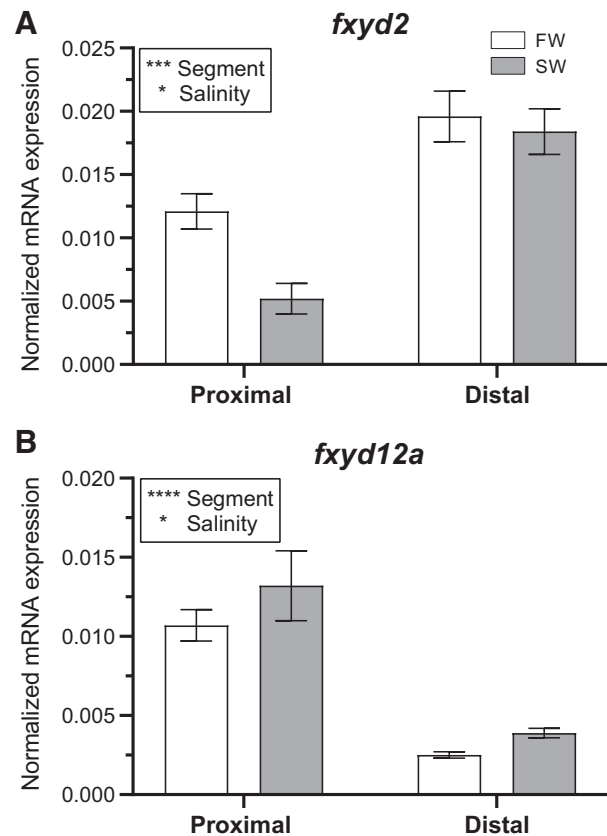


Fig. 6. Normalized mRNA levels of *fxyd* genes expressed in proximal and distal tubules microdissected from kidneys of Atlantic salmon acclimated to freshwater (FW) (white bars) or seawater (SW) (gray bars). A: *fxyd2*; B: *fxyd12a*. Inset: explanations of overall factorial effects (two-way ANOVA). Data are means  $\pm$  SE ( $n = 6$ ). \* $P < 0.05$ , \*\*\*\* $P < 0.001$ , \*\*\*\*\* $P < 0.0001$ .

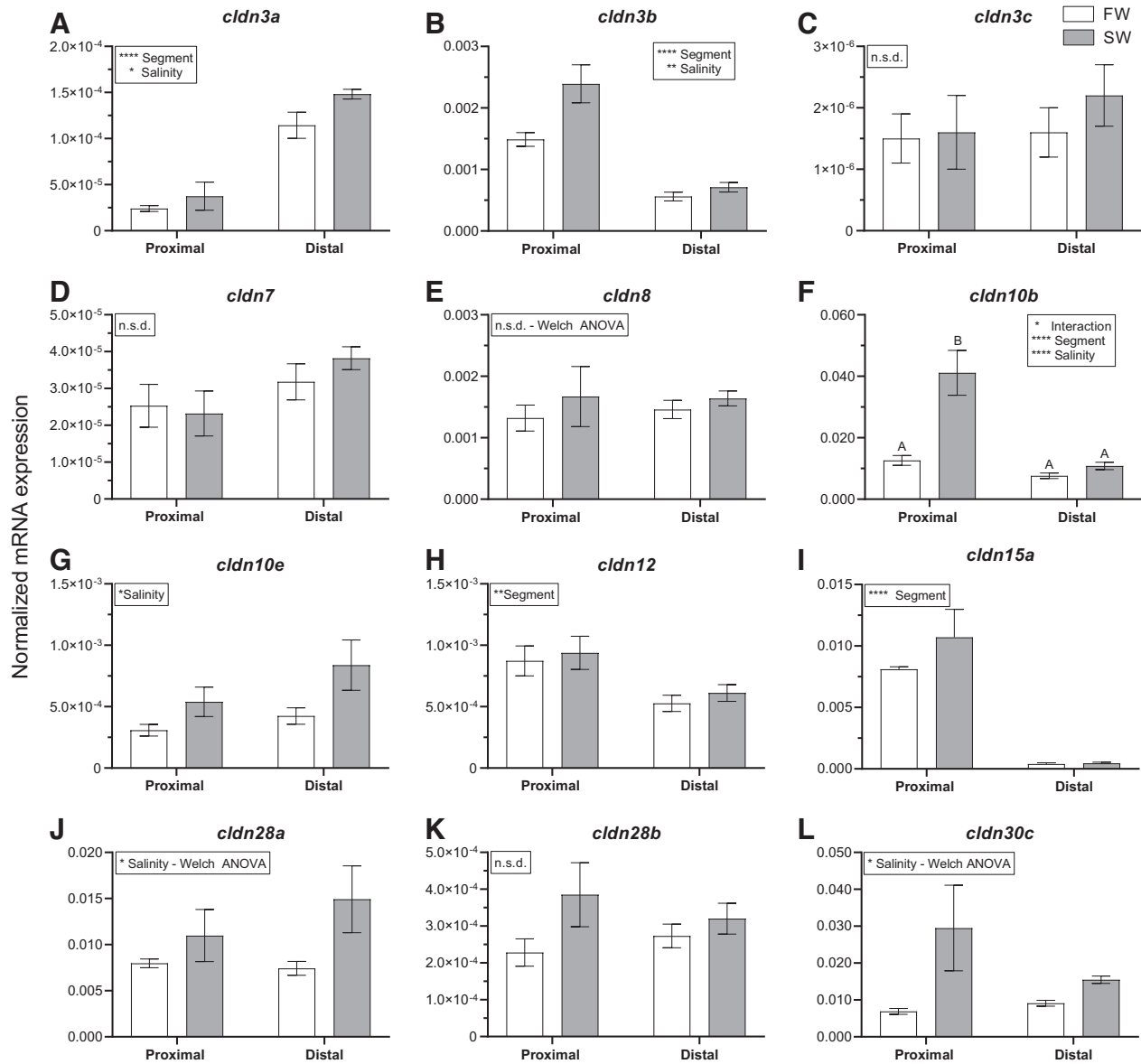


Fig. 7. Normalized mRNA levels of *claudin* genes expressed in proximal and distal tubules microdissected from kidneys of Atlantic salmon acclimated to freshwater (FW) (white bars) or seawater (SW) (gray bars). A: *cldn3a*; B: *cldn3b*; C: *cldn3c*; D: *cldn7*; E: *cldn8*; F: *cldn10b*; G: *cldn10e*; H: *cldn12*; I: *cldn15a*; J: *cldn28a*; K: *cldn28b*; L: *cldn30c*. Inset: explanations of overall factorial effects (two-way ANOVA). Data with heterogenous variance was analyzed by Welch ANOVA as indicated. In case of significant factorial interaction, post hoc multiple comparisons were made with Holm-Sidak's test. Data are means  $\pm$  SE ( $n = 6$ ). Bars sharing letters are not significantly different. \* $P < 0.05$ , \*\* $P < 0.01$ , \*\*\* $P < 0.0001$ ; n.s.d., no significant differences.

that P tubules may secrete NaCl and fluid irrespective of salinity. In FW, secreted NaCl can support elimination of water but at the same time must be reabsorbed distally and even in the bladder to not lose excessive salt. In SW, proximal secretion may add to the greatly reduced amount of filtered NaCl and provides a physiological mechanism to keep a minimal volume flow in non-filtering nephrons. Alternatively, NaCl secretion may drive a paracellular fluid flow to facilitate, e.g.,  $Mg^{2+}$  secretion, and eventually be used to reabsorb water in the D tubule onwards.

Electrophysiological measurements by Cliff and Beyenbach (20) showed that the proximal epithelium is electrically leaky, but to date renal junctional properties have not been investigated in detail in any teleost. Our data demonstrate that several claudins are expressed in the renal tubules. Claudin proteins

are important determinants of epithelial permeability by forming paired structures between adjacent cells, and several family members and paralogs are often expressed simultaneously, leading to both homo- and heterotypic structures (35, 43). It is therefore difficult to assess the overall permeability characteristics without supplementary functional measurements. However, based on homologies with the mammalian orthologs, each segment expresses both suspected barrier- and pore-forming claudins (Table 3). Another general tight junction protein is occludin, which, as the name indicates, "occludes" the paracellular pathway (32). Yet, it is interesting that  $Na^+$  pore-forming *cldn10b* and *cldn15a* are expressed at high levels in P tubules and increase nearly fourfold in SW. This suggests that this segment is a  $Na^+$ -leaky epithelium, which becomes even leakier in SW, thus supporting higher  $Na^+$  secretion in

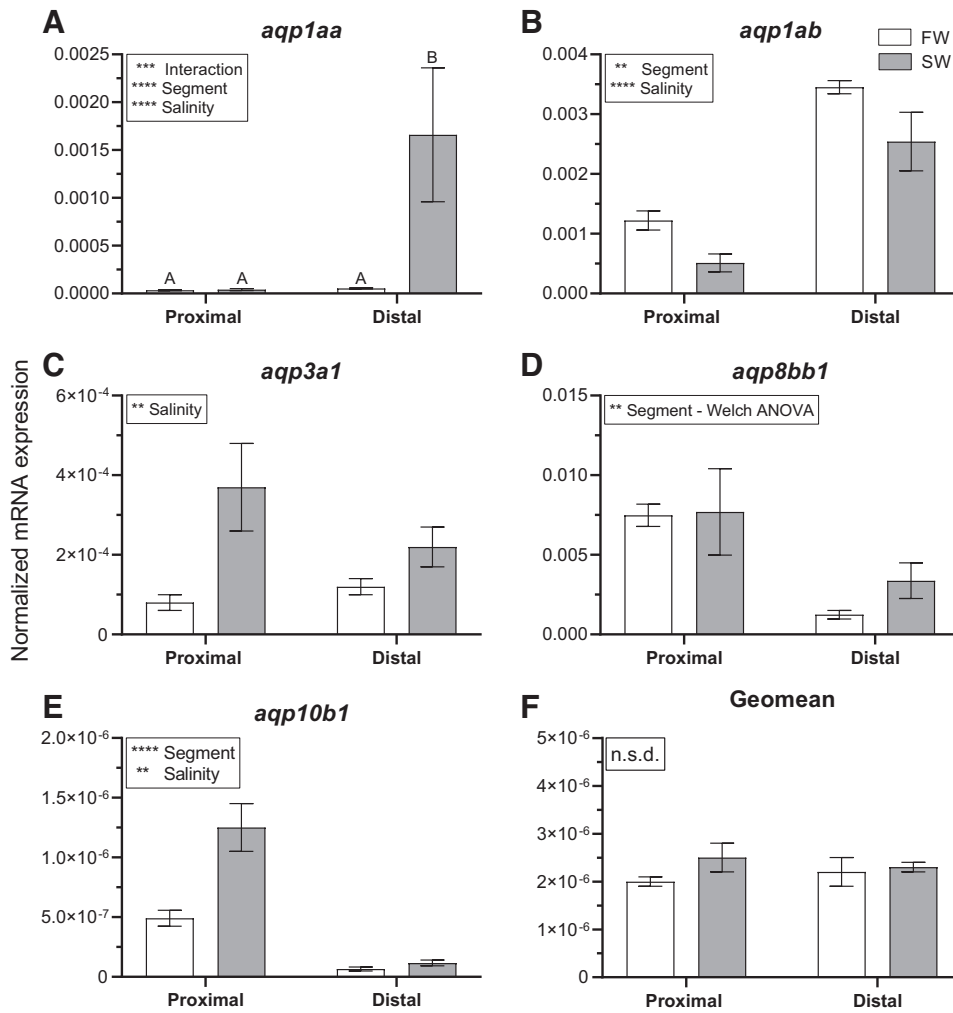


Fig. 8. Normalized mRNA levels of aquaporin genes expressed in proximal and distal tubules microdissected from kidneys of Atlantic salmon acclimated to freshwater (FW) (white bars) or seawater (SW) (gray bars). A: *aqp1aa*; B: *aqp1ab*; C: *aqp3a1*; D: *aqp8bb1*; E: *aqp10b1*; F: geometric mean (geomean). For comparison, the geomean of 3 reference genes is shown in F. Inset: explanations of overall factorial effects (two-way ANOVA). Data with heterogenous variance were analyzed by Welch ANOVA as indicated. In case of significant factorial interaction, post hoc multiple comparisons were made with Holm-Sidak's test. Data are means  $\pm$  SE ( $n = 6$ ). Bars sharing letters are not significantly different. \*\* $P < 0.01$ , \*\*\* $P < 0.001$ , \*\*\*\* $P < 0.0001$ ; n.s.d., no significant differences.

the SW kidney. Another suspected  $\text{Na}^+$  pore-forming claudin, *cldn10e*, is also more highly expressed in SW and together with the lower level of *occln* in P tubules supports a relatively leaky proximal epithelium. In the zebrafish pronephros, high levels of *occln* and *cldn8* in the distal segments also support a tightening progression through the distal tubule (64). *cldn12* may be involved in paracellular  $\text{Ca}^{2+}$  transport as in the mouse intestine (34), and our data therefore suggests that paracellular  $\text{Ca}^{2+}$  absorption may be more significant in the P tubules.

Table 3. Putative ion permeability characteristics of occludin and claudin proteins according to the references indicated

Claudin	Permeability	Reference
Claudin 3a,b,c	Cation barrier forming	(65)
Claudin 7	Anion barrier/cation pore forming	(1)
Claudin 8	Cation barrier	(91)
Claudin 10b	Cation pore	(86)
Claudin 10e	Cation pore	(60)
Claudin 12	Calcium pore	(34)
Claudin 15a	Sodium pore	(6)
Claudin 28a	Cation barrier	(77)
Claudin 28b	Cation barrier	(77)
Claudin 30c	Cation barrier	(29)
Occludin	Sealing/barrier	(32)

Another predominant transport activity in the P tubules is  $\text{Mg}^{2+}$  secretion, especially in SW conditions when the environmental  $\text{Mg}^{2+}$  load increases. The vesicular *slc41a1* Mg transporter is almost exclusively expressed in the P tubules and is strongly stimulated in SW, confirming the work by Islam et al. (46) in torafugu (*T. rubripes*). *Cnnm3* is also suspected to be involved in  $\text{Mg}^{2+}$  secretion and our data support the findings in mefugu (45) that this metal transporter is colocalized with *slc41a1* in the P tubules. However, in contrast to mefugu *cnnm3* was unchanged between FW and SW acclimated salmon.

#### Role and Regulation of NKA in Renal Tubules

At least two  $\alpha$ -subunit isoforms are expressed in the salmon kidney tubules:  $\alpha$ -1b exhibiting >1,000-fold higher transcript levels than the  $\alpha$ -1a isoform judged by calculations of relative copy numbers. Interestingly,  $\alpha$ -subunit transcript levels are unaffected by salinity, suggesting that the abundance of this enzyme is sufficient for ion transport in both conditions. However, there are salinity effects on the two regulatory *fyxd* subunits investigated. FXYD subunits are small auxiliary proteins, coexpressed and associated with the  $\alpha$ -subunit of NKA, thereby modulating its transport properties (36). Both are expressed at relatively high levels in kidney tubules (present

data and Ref. 81) and in a segment-specific manner. *fxyd2*, a kidney-specific isoform in fish (81), is expressed at highest levels in D tubules, which is similar to the expression pattern in the mammalian kidney (36). Its main effect is to reduce NKA  $V_{\max}$  and apparent affinity to  $\text{Na}^+$  and increase the affinity for ATP. *fxyd12a*, which is specifically found in fish without a mammalian ortholog, is found mainly in kidney and intestine (81, 90). It is expressed at greater than fourfold higher levels in P compared with D tubules. The precise role of Fxyd12 is unknown; however, Yang et al. (91) suggested that its association with the NKA  $\alpha$ -subunit enhanced the enzymatic activity and is thus antagonistic to the effect of Fxyd2. If this is the case, the salinity-induced effect on the two *fxyds* reinforce each other, since *fxyd2* was significantly downregulated in SW, in agreement with Tipsmark [Atlantic salmon (81)] and Yang et al. [milkfish, *Chanos chanos* (89)], while *fxyd12a* was upregulated. Nevertheless, conclusions about the net effect of FXYD proteins on the pumping activity of NKA become too speculative when merely based on transcript levels. The net effect depends on the actual stoichiometry of the translated proteins and their association with each of the two  $\alpha$ -subunit isoforms and deserves further investigation.

NKA activity forms the basis for secondary transport processes via channels and carriers. Based on studies of the salmonid gill, *nka- $\alpha$ 1a* has been termed the absorptive isoform and *nka- $\alpha$ 1b* the secretory isoform (74) even though both isoforms are located basolaterally and exhibit the same transport direction. Hence, the secondary transport they support depends solely on the presence of secondary transporters and tight junction properties and not on the basal pumping direction of the particular isoform. At present, it is unknown whether the two isoforms support opposing net transport directions in the salmonid kidney. In P tubules, NKA facilitates apical  $\text{Na}^+$ -glucose absorption and at the same time may support fluid secretion (8). In the D tubules, the prevailing function is to drive NaCl reabsorption through a combination of ion channels and cotransporters such as NKCC2, NCC, and CIC-K, which are all predominantly located here (Fig. 4, D, E, and H; Refs. 49, 66). Our data match with Wingert and Davidson (88) and McCampbell et al. (62) who used *nkcc2* and *ncc* as markers of distal segments in larval and adult zebrafish kidneys. Interestingly, these are unaffected by salinity, suggesting that transport activity by these carriers is not regulated at the transcriptional level. In the study by Kato et al. (49) NKCC2 was also not affected by salinity, whereas NCC was downregulated in distal tubules of mefugu acclimated to SW. Miyazaki et al. (66) first reported CIC-K in distal renal tubules of Mozambique tilapia (*Oreochromis mossambicus*), but in contrast to our data mRNA and protein were only detectable in FW conditions. The secretory *nkcc1* and *cftr* are also expressed in D tubules, but it is unknown to what degree they are actively contributing to NaCl secretion in this so-called “diluting segment.” It should be noted that CFTR may be involved in  $\text{Cl}^-$  reabsorption in this segment. By comparison, CFTR participates actively in  $\text{Cl}^-$  secretion in the secretory coil and in  $\text{Cl}^-$  reabsorption in the reabsorptive duct of the human sweat gland, where it is expressed apically and basolaterally, respectively (71). Higher levels of *occln* expression in combination with the presence of suspected cationic “barrier” claudins (*cldn3*, *cldn28a*, *cldn28b*, and *cldn30c*) suggest that D tubules are electrically tighter than P tubules and become even more so in SW. The transcript

profile of D tubules is characteristic of an epithelium predominantly involved in solute absorption.

#### Water Transport in Renal Tubules

Tubular processing of water is net absorptive and includes proximal secretion as well as distal reabsorption, the quantitative significance of which depends on environmental salinity. Transepithelial water transport may involve trans- as well as paracellular pathways of which the latter is mediated by aquaporin proteins (Aqp). Along the mammalian nephron, at least six isoforms are expressed in a segmental pattern and in different subcellular domains (54). By comparison, very little information exists on renal Aqps in euryhaline fishes. Paralogs of Aqp1, -3, -8, and -10 have been demonstrated in renal tissue of several euryhaline teleosts (17, 57), but there is little consensus on the role, segmental localization, and dynamics of these in fishes. Comparisons are further complicated by the great paralog diversity in the teleost lineage (16). Our study mapped the expression of five Aqps, and all, except *aqp8bb1*, are significantly affected by salinity. In the P tubules, *aqp1ab* is downregulated in SW, whereas *aqp3a1* and *-10b1* are upregulated two- to fourfold. We suggest that this upregulation facilitates fluid secretion, which is supporting the secretion of  $\text{Mg}^{2+}$  (and  $\text{SO}_4^{2-}$ ). In the D tubules, a 30-fold increase in *aqp1aa*, 2-fold increase in *aqp3a1*, and 2.7-fold increase in *aqp8bb1* in SW all support an increased fluid absorption capacity, which facilitates the formation of an isotonic urine. The salinity effects are overall in full agreement with the earlier report by Tipsmark et al. (84) based on whole kidney analyses. Other studies using whole kidney homogenates have shown the following: increase [European sea bass (38, 39); Indian ricefish, *Oryzias dancena* (51)] or decrease [European eel, *Anguilla* (61); Black porgy, *Acanthopagrus schlegeli* (4)] in *aqp1* paralogs in SW and increase in *aqp3b* [European eel (22)] and *aqp3a* in SW (Mozambique tilapia (87)] or decrease in *aqp10b* in SW [European eel (61)]. Thus there is very little consensus between studies, which may in part be explained by species variation, the use of whole kidney homogenates and lack of segment-specific information. We have previously reported the localization of Aqp1aa, -1ab, and -8bb1 in P tubules of rainbow trout (27, 28), and Aqp3 was previously found apically in “undefined renal tubules” of silver eels (22). Paracellular water transport through claudin-based water pores may supplement Aqp-mediated water transport. E.g. has it been documented that Cldn2 and Cldn15 may create water pores in the mouse proximal renal tubules and small intestine, respectively (75, 76). Cldn2 has not been reported in salmon thus far (69), and the permeability properties of Cldn15 are unknown.

#### Conclusions and Perspectives

This study provides deep insight into the segmental localization and expression dynamics of important solute- and water-transport proteins in a euryhaline fish kidney in relation to the major transition between a water-load and a water-deficiency situation created by the environment. The data outline major differences in transcript profiles between proximal and distal tubules and give evidence that regulation at the transcriptional level contributes significantly to the switch in kidney function between these environments. Since glomerular

intermittency is prevalent in fish kidneys, future studies should aim at clarifying whether perfused and non-perfused tubules are regulated differently.

#### GRANTS

This project was funded by Danish Research Council for Independent Research Grant DFF-4181-00020 (to S. S. Madsen).

#### DISCLOSURES

No conflicts of interest, financial or otherwise, are declared by the authors.

#### AUTHOR CONTRIBUTIONS

S.S.M. and R.J.B. conceived and designed research; R.J.B., M.B., and M.B.E. performed experiments; S.S.M. and R.J.B. analyzed data; S.S.M. interpreted results of experiments; R.J.B. prepared figures; S.S.M. drafted manuscript; S.S.M., R.J.B., M.B., and M.B.E. edited and revised manuscript; S.S.M., R.J.B., M.B., and M.B.E. approved final version of manuscript.

#### REFERENCES

- Alexandre MD, Lu Q, Chen YH. Overexpression of claudin-7 decreases the paracellular  $\text{Cl}^-$  conductance and increases the paracellular  $\text{Na}^+$  conductance in LLC-PK1 cells. *J Cell Sci* 118: 2683–2693, 2005. doi:10.1242/jcs.02406.
- Althoff T, Hentschel H, Luig J, Schütz H, Kasch M, Kinne RK.  $\text{Na}^+$ -D-glucose cotransporter in the kidney of *Squalus acanthias*: molecular identification and intrarenal distribution. *Am J Physiol Regul Integr Comp Physiol* 290: R1094–R1104, 2006. doi:10.1152/ajpregu.00334.2005.
- Althoff T, Hentschel H, Luig J, Schütz H, Kasch M, Kinne RK.  $\text{Na}^+$ -D-glucose cotransporter in the kidney of *Leucoraja erinacea*: molecular identification and intrarenal distribution. *Am J Physiol Regul Integr Comp Physiol* 292: R2391–R2399, 2007. doi:10.1152/ajpregu.00454.2006.
- An KW, Kim NN, Choi CY. Cloning and expression of aquaporin 1 and arginine vasotocin receptor mRNA from the black porgy, *Acanthopagrus schlegelii*: effect of freshwater acclimation. *Fish Physiol Biochem* 34: 185–194, 2008. doi:10.1007/s10695-007-9175-0.
- Anderson BG, Loewen RD. Renal morphology of freshwater trout. *Am J Anat* 143: 93–113, 1975. doi:10.1002/aja.1001430105.
- Bagnat M, Cheung ID, Mostov KE, Stainier DY. Genetic control of single lumen formation in the zebrafish gut. *Nat Cell Biol* 9: 954–960, 2007. doi:10.1038/ncb1621.
- Bas A, Forsberg G, Hammarström S, Hammarström ML. Utility of the housekeeping genes 18S rRNA, beta-actin and glyceraldehyde-3-phosphate-dehydrogenase for normalization in real-time quantitative reverse transcriptase-polymerase chain reaction analysis of gene expression in human T lymphocytes. *Scand J Immunol* 59: 566–573, 2004. doi:10.1111/j.0300-9475.2004.01440.x.
- Beyenbach KW. Kidneys sans glomeruli. *Am J Physiol Renal Physiol* 286: F811–F827, 2004. doi:10.1152/ajprenal.00351.2003.
- Beyenbach KW. Renal handling of magnesium in fish: from whole animal to brush border membrane vesicles. *Front Biosci* 5: D712–D719, 2000. doi:10.2741/beyenbach.
- Bodinier C, Boulo V, Lorin-Nebel C, Charmantier G. Influence of salinity on the localization and expression of the CFTR chloride channel in the ionocytes of *Dicentrarchus labrax* during ontogeny. *J Anat* 214: 318–329, 2009. doi:10.1111/j.1469-7580.2009.01050.x.
- Bossus MC, Madsen SS, Tipsmark CK. Functional dynamics of claudin expression in Japanese medaka (*Oryzias latipes*): response to environmental salinity. *Comp Biochem Physiol A Mol Integr Physiol* 187: 74–85, 2015. doi:10.1016/j.cbpa.2015.04.017.
- Boyle D, Clifford AM, Orr E, Chamot D, Goss GG. Mechanisms of  $\text{Cl}^-$  uptake in rainbow trout: cloning and expression of slc26a6, a prospective  $\text{Cl}^-/\text{HCO}_3^-$  exchanger. *Comp Biochem Physiol A Mol Integr Physiol* 180: 43–50, 2015. doi:10.1016/j.cbpa.2014.11.001.
- Braun EJ, Dantzer WH. Vertebrate renal system. In: *Handbook of Physiology: Comparative Physiology*, edited by Dantzer WH. Oxford: Oxford University Press, 1997, vol 1, p. 481–576. doi:10.1002/cphy.cp130108.
- Brown JA, Jackson BA, Oliver JA, Henderson IW. Single nephron filtration rates (SNGFR) in the trout, *Salmo gairdneri*. Validation of the use of ferrocyanide and the effects on environmental salinity. *Pflügers Arch* 377: 101–108, 1978. doi:10.1007/BF00584381.
- Brown JA, Oliver JA, Henderson IW, Jackson BA. Angiotensin and single nephron glomerular function in the trout *Salmo gairdneri*. *Am J Physiol* 239: R509–R514, 1980. doi:10.1152/ajpregu.1980.239.5.R509.
- Bucking C, Wood CM. Renal regulation of plasma glucose in the freshwater rainbow trout. *J Exp Biol* 208: 2731–2739, 2005. doi:10.1242/jeb.01668.
- Cerdà J, Finn RN. Piscine aquaporins: an overview of recent advances. *J Exp Zool A Ecol Genet Physiol* 313A: 623–650, 2010. doi:10.1002/jez.634.
- Chandra S, Morrison GH, Beyenbach KW. Identification of Mg-transporting renal tubules and cells by ion microscopy imaging of stable isotopes. *Am J Physiol* 273: F939–F948, 1997. doi:10.1152/ajprenal.1997.273.6.F939.
- Chasiotis H, Kelly SP. Occludin immunolocalization and protein expression in goldfish. *J Exp Biol* 211: 1524–1534, 2008. doi:10.1242/jeb.014894.
- Cliff WH, Beyenbach KW. Secretory renal proximal tubules in seawater- and freshwater-adapted killifish. *Am J Physiol Renal Physiol* 262: F108–F116, 1992. doi:10.1152/ajprenal.1992.262.1.F108.
- Cutler CP, Cramb G. Two isoforms of the  $\text{Na}^+/\text{K}^+/\text{2Cl}^-$  cotransporter are expressed in the European eel (*Anguilla anguilla*). *Biochim Biophys Acta* 1566: 92–103, 2002. doi:10.1016/S0005-2736(02)00596-5.
- Cutler CP, Martinez AS, Cramb G. The role of aquaporin 3 in teleost fish. *Comp Biochem Physiol A Mol Integr Physiol* 148: 82–91, 2007. doi:10.1016/j.cbpa.2006.09.022.
- Dantzer WH. Regulation of renal proximal and distal tubule transport: sodium, chloride and organic anions. *Comp Biochem Physiol A Mol Integr Physiol* 136: 453–478, 2003. doi:10.1016/S1095-6433(03)00135-1.
- Elger M, Kaune R, Hentschel H. Glomerular intermittency in a freshwater teleost, *Carassius auratus gibelio*, after transfer to salt water. *Am J Physiol Renal Physiol* 154: 225–231, 1984. doi:10.1007/BF02464400.
- Ellis LV, Bollinger RJ, Weber HM, Madsen SS, Tipsmark CK. Differential expression and localization of branchial AQP1 and AQP3 in Japanese medaka (*Oryzias latipes*). *Cells* 8: 422, 2019. doi:10.3390/cells8050422.
- Engelund MB, Chauvigné F, Christensen BM, Finn RN, Cerdà J, Madsen SS. Differential expression and novel permeability properties of three aquaporin 8 paralogs from seawater-challenged Atlantic salmon smolts. *J Exp Biol* 216: 3873–3885, 2013. doi:10.1242/jeb.087890.
- Engelund MB, Madsen SS. The role of aquaporins in the kidney of euryhaline teleosts. *Front Physiol* 2: 51, 2011. doi:10.3389/fphys.2011.00051.
- Engelund MB, Madsen SS. Tubular localization and expression dynamics of aquaporins in the kidney of seawater-challenged Atlantic salmon. *J Comp Physiol B* 185: 207–223, 2015. doi:10.1007/s00360-014-0878-0.
- Engelund MB, Yu ASL, Li J, Madsen SS, Færgeman NJ, Tipsmark CK. Functional characterization and localization of a gill-specific claudin isoform in Atlantic salmon. *Am J Physiol Regul Integr Comp Physiol* 302: R300–R311, 2012. doi:10.1152/ajpregu.00286.2011.
- Espina V, Wulffkuhle JD, Calvert VS, VanMeter A, Zhou W, Coukos G, Geho DH, Petricoin EF 3rd, Liotta LA. Laser-capture microdissection. *Nat Protoc* 1: 586–603, 2006. doi:10.1038/nprot.2006.85.
- Evans DH, Piermarini PM, Choe KP. The multifunctional fish gill: dominant site of gas exchange, osmoregulation, acid-base regulation, and excretion of nitrogenous waste. *Physiol Rev* 85: 97–177, 2005. doi:10.1152/physrev.00050.2003.
- Feldman GJ, Mullin JM, Ryan MP. Occludin: structure, function and regulation. *Adv Drug Deliv Rev* 57: 883–917, 2005. doi:10.1016/j.addr.2005.01.009.
- Freire CA, Kinne-Saffran E, Beyenbach KW, Kinne RK.  $\text{Na}^+$ -D-glucose cotransport in renal brush-border membrane vesicles of an early teleost (*Oncorhynchus mykiss*). *Am J Physiol Regul Integr Comp Physiol* 269: R592–R602, 1995. doi:10.1152/ajpregu.1995.269.3.R592.
- Fujita H, Sugimoto K, Inatomi S, Maeda T, Osanai M, Uchiyama Y, Yamamoto Y, Wada T, Kojima T, Yokozaki H, Yamashita T, Kato S, Sawada N, Chiba H. Tight junction proteins claudin-2 and -12 are critical for vitamin D-dependent  $\text{Ca}^{2+}$  absorption between enterocytes. *Mol Biol Cell* 19: 1912–1921, 2008. doi:10.1091/mbc.e07-09-0973.
- Furuse M, Sasaki H, Tsukita S. Manner of interaction of heterogeneous claudin species within and between tight junction strands. *J Cell Biol* 147: 891–903, 1999. doi:10.1083/jcb.147.4.891.

36. Geering K. FXYP proteins: new regulators of Na-K-ATPase. *Am J Physiol Renal Physiol* 290: F241–F250, 2006. doi:10.1152/ajprenal.00126.2005.
37. Giffard-Mena I, Boulo V, Abed C, Cramb G, Charmantier G. Expression and localization of aquaporin 1a in the sea-bass (*Dicentrarchus labrax*) during ontogeny. *Front Physiol* 2: 34, 2011. doi:10.3389/fphys.2011.00034.
38. Genz J, Esbaugh AJ, Grosell M. Intestinal transport following transfer to increased salinity in an anadromous fish (*Oncorhynchus mykiss*). *Comp Biochem Physiol A Mol Integr Physiol* 159: 150–158, 2011. doi:10.1016/j.cbpa.2011.02.011.
39. Giffard-Mena I, Boulo V, Aujoulat F, Fowden H, Castille R, Charmantier G, Cramb G. Aquaporin molecular characterization in the sea-bass (*Dicentrarchus labrax*): the effect of salinity on AQP1 and AQP3 expression. *Comp Biochem Physiol A Mol Integr Physiol* 148: 430–444, 2007. doi:10.1016/j.cbpa.2007.06.002.
40. Günzel D, Yu AS. Claudins and the modulation of tight junction permeability. *Physiol Rev* 93: 525–569, 2013. doi:10.1152/physrev.00019.2012.
41. Hickman CP, Trump BF. The kidney. In: *Fish Physiology*, edited by Hoar WS, Randall DJ. New York: Academic, 1969, vol. 1, p. 99–239.
42. Hiroi J, McCormick SD, Ohtani-Kaneko R, Kaneko T. Functional classification of mitochondrion-rich cells in euryhaline Mozambique tilapia (*Oreochromis mossambicus*) embryos, by means of triple immunofluorescence staining for Na<sup>+</sup>/K<sup>+</sup>-ATPase, Na<sup>+</sup>/K<sup>+</sup>/2Cl<sup>-</sup> cotransporter and CFTR anion channel. *J Exp Biol* 208: 2023–2036, 2005. doi:10.1242/jeb.01611.
43. Hou J, Rajagopal M, Yu AS. Claudins and the kidney. *Annu Rev Physiol* 75: 479–501, 2013. doi:10.1146/annurev-physiol-030212-183705.
44. Hwang PP, Lee TH, Lin LY. Ion regulation in fish gills: recent progress in the cellular and molecular mechanisms. *Am J Physiol Regul Integr Comp Physiol* 301: R28–R47, 2011. doi:10.1152/ajpregu.00047.2011.
45. Islam Z, Hayashi N, Inoue H, Umezawa T, Kimura Y, Doi H, Romero MF, Hirose S, Kato A. Identification and lateral membrane localization of cyclin M3, likely to be involved in renal Mg<sup>2+</sup> handling in seawater fish. *Am J Physiol Regul Integr Comp Physiol* 307: R525–R537, 2014. doi:10.1152/ajpregu.00032.2014.
46. Islam Z, Hayashi N, Yamamoto Y, Doi H, Romero MF, Hirose S, Kato A. Identification and proximal tubular localization of the Mg<sup>2+</sup> transporter, Slc41a1, in a seawater fish. *Am J Physiol Regul Integr Comp Physiol* 305: R385–R396, 2013. doi:10.1152/ajpregu.00507.2012.
47. Ivanis G, Braun M, Perry SF. Renal expression and localization of SLC9A3 sodium/hydrogen exchanger and its possible role in acid-base regulation in freshwater rainbow trout (*Oncorhynchus mykiss*). *Am J Physiol Regul Integr Comp Physiol* 295: R971–R978, 2008. doi:10.1152/ajpregu.90328.2008.
48. Kato A, Chang MH, Kurita Y, Nakada T, Ogoshi M, Nakazato T, Doi H, Hirose S, Romero MF. Identification of renal transporters involved in sulfate excretion in marine teleost fish. *Am J Physiol Regul Integr Comp Physiol* 297: R1647–R1659, 2009. doi:10.1152/ajpregu.00228.2009.
49. Kato A, Muro T, Kimura Y, Li S, Islam Z, Ogoshi M, Doi H, Hirose S. Differential expression of Na<sup>+</sup>-Cl<sup>-</sup> cotransporter and Na<sup>+</sup>-K<sup>+</sup>-Cl<sup>-</sup> cotransporter 2 in the distal nephrons of euryhaline and seawater pufferfishes. *Am J Physiol Regul Integr Comp Physiol* 300: R284–R297, 2011. doi:10.1152/ajpregu.00725.2009.
50. Katoh F, Cozzi RR, Marshall WS, Goss GG. Distinct Na<sup>+</sup>/K<sup>+</sup>/2Cl<sup>-</sup> cotransporter localization in kidneys and gills of two euryhaline species, rainbow trout and killifish. *Cell Tissue Res* 334: 265–281, 2008. doi:10.1007/s00441-008-0679-4.
51. Kim YK, Lee SY, Kim BS, Kim DS, Nam YK. Isolation and mRNA expression analysis of aquaporin isoforms in marine medaka *Oryzias latipes*, a euryhaline teleost. *Comp Biochem Physiol A Mol Integr Physiol* 171: 1–8, 2014. doi:10.1016/j.cbpa.2014.01.012.
52. Kolosov D, Bui P, Chasiotis H, Kelly SP. Claudins in teleost fishes. *Tissue Barriers* 1: e25391, 2013. doi:10.4161/tisb.25391.
53. Koressaar T, Remm M. Enhancements and modifications of primer design program Primer3. *Bioinformatics* 23: 1289–1291, 2007. doi:10.1093/bioinformatics/btm091.
54. Kortenoeven MLA, Fenton RA. Renal aquaporins and water balance disorders. *Biochim Biophys Acta* 1840: 1533–1549, 2014. doi:10.1016/j.bbagen.2013.12.002.
55. Krebs S, Fischaleck M, Blum H. A simple and loss-free method to remove TRIzol contaminations from minute RNA samples. *Anal Biochem* 387: 136–138, 2009. doi:10.1016/j.ab.2008.12.020.
56. Madsen SS, Bujak J, Tipsmark CK. Aquaporin expression in the Japanese medaka (*Oryzias latipes*) in freshwater and seawater: challenging the paradigm of intestinal water transport? *J Exp Biol* 217: 3108–3121, 2014. doi:10.1242/jeb.105098.
57. Madsen SS, Engelund MB, Cutler CP. Water transport and functional dynamics of aquaporins in osmoregulatory organs of fishes. *Biol Bull* 229: 70–92, 2015. doi:10.1086/BBLv229n1p70.
58. Madsen SS, Kiilerich P, Tipsmark CK. Multiplicity of expression of Na<sup>+</sup>,K<sup>+</sup>-ATPase  $\alpha$ -subunit isoforms in the gill of Atlantic salmon (*Salmo salar*): cellular localisation and absolute quantification in response to salinity change. *J Exp Biol* 212: 78–88, 2009. doi:10.1242/jeb.024612.
59. Marshall WS. Transport processes in isolated teleost epithelia: opercular epithelium and urinary bladder. *Fish Physiol* 14: 1–23, 1995. doi:10.1016/S1546-5098(08)60240-X.
60. Marshall WS, Breves JP, Doohan EM, Tipsmark CK, Kelly SP, Robertson GN, Schulte PM. claudin-10 isoform expression and cation selectivity change with salinity in salt-secreting epithelia of *Fundulus heteroclitus*. *J Exp Biol* 221: jeb168906, 2018. doi:10.1242/jeb.168906.
61. Martínez AS, Cutler CP, Wilson GD, Phillips C, Hazon N, Cramb G. Cloning and expression of three aquaporin homologues from the European eel (*Anguilla anguilla*): effects of seawater acclimation and cortisol treatment on renal expression. *Biol Cell* 97: 615–627, 2005. doi:10.1042/BC20040111.
62. McCampbell KK, Springer KN, Wingert RA. Analysis of nephron composition and function in the adult zebrafish kidney. *J Vis Exp* 90: e51644, 2014. doi:10.3791/51644.
63. McDonald MD. The renal contribution to salt and water balance. In: *Fish Osmoregulation*, edited by Baldisserotto B, Romero JM, Kapoor BG. Enfield, NH: Science Publishers, 2007, p. 322–345.
64. McKee R, Gerlach GF, Jou J, Cheng CN, Wingert RA. Temporal and spatial expression of tight junction genes during zebrafish pronephros development. *Gene Expr Patterns* 16: 104–113, 2014. doi:10.1016/j.gep.2014.11.001.
65. Milatz S, Krug SM, Rosenthal R, Günzel D, Müller D, Schulzke JD, Amasheh S, Fromm M. Claudin-3 acts as a sealing component of the tight junction for ions of either charge and uncharged solutes. *Biochim Biophys Acta* 1798: 2048–2057, 2010. doi:10.1016/j.bbame.2010.07.014.
66. Miyazaki H, Kaneko T, Uchida S, Sasaki S, Takei Y. Kidney-specific chloride channel, OmClC-K, predominantly expressed in the diluting segment of freshwater-adapted tilapia kidney. *Proc Natl Acad Sci USA* 99: 15782–15787, 2002. doi:10.1073/pnas.242611099.
67. Nishimura H, Imai M. Control of renal function in freshwater and marine teleosts. *Fed Proc* 41: 2355–2360, 1982.
68. Nishimura H, Imai M, Ogawa M. Sodium chloride and water transport in the renal distal tubule of the rainbow trout. *Am J Physiol Renal Physiol* 244: F247–F254, 1983. doi:10.1152/ajprenal.1983.244.3.F247.
69. Pfaffl MW. A new mathematical model for relative quantification in real-time RT-PCR. *Nucleic Acids Res* 29: 45e, 2001. doi:10.1093/nar/29.9.e45.
70. Polakof S, Álvarez R, Soengas JL. Gut glucose metabolism in rainbow trout: implications in glucose homeostasis and glucosensing capacity. *Am J Physiol Regul Integr Comp Physiol* 299: R19–R32, 2010. doi:10.1152/ajpregu.00005.2010.
71. Quinton PM. Cystic fibrosis: lessons from the sweat gland. *Physiology (Bethesda)* 22: 212–225, 2007. doi:10.1152/physiol.00041.2006.
72. Renfro JL. Recent developments in teleost renal transport. *J Exp Zool* 283: 653–661, 1999. doi:10.1002/(SICI)1097-010X(19990601)283:7<653::AID-JEZ4>3.0.CO;2-M.
73. Resende AD, Lobo-da-Cunha A, Malhão F, Franquinho F, Monteiro RA, Rocha E. Histological and stereological characterization of brown trout (*Salmo trutta f. fario*) trunk kidney. *Microsc Microanal* 16: 677–687, 2010. doi:10.1017/S1431927610093918.
74. Richards JG, Semple JW, Bystriansky JS, Schulte PM. Na<sup>+</sup>/K<sup>+</sup>-ATPase alpha-isoform switching in gills of rainbow trout (*Oncorhynchus mykiss*) during salinity transfer. *J Exp Biol* 206: 4475–4486, 2003. doi:10.1242/jeb.00701.
75. Rosenthal R, Günzel D, Piontek J, Krug SM, Ayala-Torres C, Hempel C, Theune D, Fromm M. Claudin-15 forms a water channel through the tight junction with distinct function compared to claudin-2. *Acta Physiol (Oxf)* 228: e13334, 2020. doi:10.1111/apha.13334.
76. Rosenthal R, Milatz S, Krug SM, Oelrich B, Schulzke JD, Amasheh S, Günzel D, Fromm M. Claudin-2, a component of the tight junction, forms

- a paracellular water channel. *J Cell Sci* 123: 1913–1921, 2010. doi:10.1242/jcs.060665.
77. **Sandbichler AM, Egg M, Schwerte T, Pelster B.** Claudin 28b and F-actin are involved in rainbow trout gill pavement cell tight junction remodeling under osmotic stress. *J Exp Biol* 214: 1473–1487, 2011. doi:10.1242/jeb.050062.
  78. **Souza-Menezes J, Morales MM.** CFTR structure and function: is there a role in the kidney? *Biophys Rev* 1: 3–12, 2009. doi:10.1007/s12551-008-0002-3.
  79. **Sundell KS, Sundh H.** Intestinal fluid absorption in anadromous salmonids: importance of tight junctions and aquaporins. *Front Physiol* 3: 388, 2012. doi:10.3389/fphys.2012.00388.
  80. **Teranishi K, Kaneko T.** Spatial, cellular, and intracellular localization of Na<sup>+</sup>/K<sup>+</sup>-ATPase in the sterically disposed renal tubules of Japanese eel. *J Histochem Cytochem* 58: 707–719, 2010. doi:10.1369/jhc.2010.955492.
  81. **Tipmark CK.** Identification of FXFD protein genes in a teleost: tissue-specific expression and response to salinity change. *Am J Physiol Regul Integr Comp Physiol* 294: R1367–R1378, 2008. doi:10.1152/ajpregu.00454.2007.
  82. **Tipmark CK, Küllerich P, Nilsen TO, Ebbesson LO, Stefansson SO, Madsen SS.** Branchial expression patterns of claudin isoforms in Atlantic salmon during seawater acclimation and smoltification. *Am J Physiol Regul Integr Comp Physiol* 294: R1563–R1574, 2008. doi:10.1152/ajpregu.00915.2007.
  83. **Tipmark CK, Madsen SS.** Distinct hormonal regulation of Na<sup>+</sup>,K<sup>+</sup>-atpase genes in the gill of Atlantic salmon (*Salmo salar* L.). *J Endocrinol* 203: 301–310, 2009. doi:10.1677/JOE-09-0281.
  84. **Tipmark CK, Sørensen KJ, Madsen SS.** Aquaporin expression dynamics in osmoregulatory tissues of Atlantic salmon during smoltification and seawater acclimation. *J Exp Biol* 213: 368–379, 2010. doi:10.1242/jeb.034785.
  85. **Tipmark CK, Madsen SS.** Tricellulin, occludin and claudin-3 expression in salmon intestine and kidney during salinity adaptation. *Comp Biochem Physiol A Mol Integr Physiol* 162: 378–385, 2012. doi:10.1016/j.cbpa.2012.04.020.
  86. **Van Itallie CM, Rogan S, Yu A, Vidal LS, Holmes J, Anderson JM.** Two splice variants of claudin-10 in the kidney create paracellular pores with different ion selectivities. *Am J Physiol Renal Physiol* 291: F1288–F1299, 2006. doi:10.1152/ajprenal.00138.2006.
  87. **Watanabe S, Kaneko T, Aida K.** Aquaporin-3 expressed in the basolateral membrane of gill chloride cells in Mozambique tilapia *Oreochromis mossambicus* adapted to freshwater and seawater. *J Exp Biol* 208: 2673–2682, 2005. doi:10.1242/jeb.01684.
  88. **Wingert RA, Davidson AJ.** Zebrafish nephrogenesis involves dynamic spatiotemporal expression changes in renal progenitors and essential signals from retinoic acid and irx3b. *Dev Dyn* 240: 2011–2027, 2011. doi:10.1002/dvdy.22691.
  89. **Yang W, Chao T, Chuang H, Hu Y, Lorin-Nebel C, Blondeau-Bidet E, Wu W, Tang C, Tsai S, Lee T.** Gene expression of Na<sup>+</sup>/K<sup>+</sup>-ATPase  $\alpha$ -isoforms and FXFD proteins and potential modulatory mechanisms in euryhaline milkfish kidneys upon hypoosmotic challenges. *Aquaculture* 504: 59–69, 2019. doi:10.1016/j.aquaculture.2019.01.046.
  90. **Yang WK, Kang CK, Hsu AD, Lin CH, Lee TH.** Different modulatory mechanisms of renal FXFD12 for Na<sup>+</sup>,K<sup>+</sup>-ATPase between two closely related medakas upon salinity challenge. *Int J Biol Sci* 12: 730–745, 2016. doi:10.7150/ijbs.15066.
  91. **Yu AS, Enck AH, Lencer WL, Schneeberger EE.** Claudin-8 expression in Madin-Darby canine kidney cells augments the paracellular barrier to cation permeation. *J Biol Chem* 278: 17350–17359, 2003. doi:10.1074/jbc.M213286200.